




OPEN

# Lack of alpha CGRP exacerbates the development of atherosclerosis in ApoE-knockout mice

Narumi Hashikawa-Hobara , Shota Inoue & Naoya Hashikawa

The effects of calcitonin gene-related peptide (CGRP) on atherosclerosis remain unclear. We used apolipoprotein E-deficient (*ApoE*<sup>-/-</sup>) mice to generate double-knockout *ApoE*<sup>-/-</sup>:*CGRP*<sup>-/-</sup> mice lacking alpha CGRP. *ApoE*<sup>-/-</sup>:*CGRP*<sup>-/-</sup> mice exhibited larger atherosclerotic plaque areas, peritoneal macrophages with enhanced migration functions, and elevated levels of the inflammatory cytokine tumor necrosis factor (TNF)- $\alpha$ . Thus, we also explored whether inhibiting TNF- $\alpha$  could improve atherosclerosis in *ApoE*<sup>-/-</sup>:*CGRP*<sup>-/-</sup> mice by administering etanercept intraperitoneally once a week (5 mg/kg) alongside a high-fat diet for 2 weeks. This treatment led to significant reductions in aortic root lesion size, atherosclerotic plaque area and macrophage migration in *ApoE*<sup>-/-</sup>:*CGRP*<sup>-/-</sup> mice compared with mice treated with human IgG (5 mg/kg). We further examined whether results observed in *ApoE*<sup>-/-</sup>:*CGRP*<sup>-/-</sup> mice could similarly be obtained by administering a humanized monoclonal CGRP antibody, galcanezumab, to *ApoE*<sup>-/-</sup> mice. *ApoE*<sup>-/-</sup> mice were subcutaneously administered galcanezumab at an initial dose of 50 mg/kg, followed by a dose of 30 mg/kg in the second week. Galcanezumab administration did not affect systolic blood pressure, serum lipid levels, or macrophage migration but led to a significant increase in lipid deposition at the aortic root. These findings suggest that alpha CGRP plays a critical role in inhibiting the progression of atherosclerosis.

Calcitonin gene-related peptide (CGRP), a potent vasodilator<sup>1</sup>, is a 37-residue amino acid produced by alternative splicing of the calcitonin gene<sup>2</sup>. There are two types of CGRP,  $\alpha$ CGRP and  $\beta$ CGRP. The gene name for  $\alpha$ CGRP in mice is '*Calca*', which codes for the alpha calcitonin-related peptide<sup>3,4</sup>. Throughout the present study, we have uniformly used the term CGRP to maintain consistency. CGRP is involved in detection by central and peripheral capsaicin-sensitive nerves and has a pivotal role in regulating peripheral vascular tone<sup>5,6</sup>. Additionally, CGRP plays an anti-inflammatory role in immune reactions by inhibiting lipopolysaccharide (LPS)-induced release of interleukin (IL)-1 $\beta$  and tumor necrosis factor (TNF)- $\alpha$  in osteoblasts<sup>7</sup>. A study of mice deficient for a component of CGRP receptors (receptor activity-modifying protein 1, *RAMP1*<sup>-/-</sup>) demonstrated the involvement of CGRP receptors in regulation of proinflammatory cytokine production<sup>8</sup>. Furthermore, exogenous administration of CGRP reportedly inhibits infiltration of macrophages and expression of various inflammatory mediators, such as nuclear factor kappa B (NF- $\kappa$ B), IL-1 $\beta$ , TNF- $\alpha$ , inducible nitric oxide synthase, matrix metalloproteinase 9, and intercellular adhesion molecule 1, thus attenuating the consequences of inflammation<sup>9-11</sup>.

Atherosclerosis is considered a chronic and progressive inflammatory disease that largely depends on macrophages to promote inflammation<sup>12</sup>. Previous studies show that transient receptor potential vanilloid subfamily member 1 (TRPV1), which can promote release of CGRP, inhibits inflammation by activating phosphatidylinositol 3 kinase (PI3K)/Akt signaling and suppressing activation of NF- $\kappa$ B<sup>13,14</sup>. Although accumulating evidence suggests that CGRP has a protective effect against inflammation, how CGRP is involved in atherosclerotic lesions is less well understood. To define the precise role that CGRP plays in atherogenesis, we used a newly generated double-knockout mouse line in which both CGRP and apolipoprotein E (*ApoE*) are deleted. These mice were fed a high-fat diet (HFD) and analyzed for atherosclerotic lesion formation and peritoneal macrophage functions. In addition, we evaluated whether a TNF- $\alpha$  inhibitor previously reported to have beneficial effects in subclinical atherosclerosis<sup>15</sup> would be effective in preventing the progression of atherosclerosis in our double-knockout mice. Moreover, we examined whether administration of a humanized IgG4 monoclonal antibody that binds CGRP (galcanezumab) to *ApoE*-knockout (*ApoE*<sup>-/-</sup>) mice could affect atherosclerotic lesions and peritoneal macrophage functions.

Department of Life Science, Okayama University of Science, 1-1 Ridai-Cho, Kita-Ku, Okayama 700-0005, Japan.  
✉ email: hashikawa-hobara@ous.ac.jp

**Figure 1.** CGRP deficiency is associated with increased atherosclerotic lesion area. (a) Administering a high-fat diet (HFD) for 10-week to C57BL6J, *ApoE*<sup>-/-</sup>, *CGRP*<sup>-/-</sup> or *ApoE*<sup>-/-</sup>:*CGRP*<sup>-/-</sup> mice and evaluating atherosclerotic lesions. (b) Representative photomicrographs of aortic lesions stained with Oil Red O. (c) Quantification of atherosclerotic lesions in the aortic arch by Oil red-O staining from wild-type mice (n = 13), apolipoprotein E-deficient (*ApoE*<sup>-/-</sup>) mice (n = 12), *CGRP*<sup>-/-</sup> mice (n = 4), and *ApoE*<sup>-/-</sup>:*CGRP*<sup>-/-</sup> mice (n = 10) fed a high-fat diet (HFD) for 10 weeks. (d) Quantification of atherosclerotic lesions in the thoracic aorta. (e) Quantification of atherosclerotic lesions in the abdominal area of aorta. Scale bar indicates 2 mm. (f) Photomicrographs of aortic sinus lesions from mice fed a HFD for 10 weeks with Oil Red O staining. (g) Eight-week-old mice were fed a HFD for 1 week before the peritoneal macrophage assay was performed. (h) Numbers of adherent peritoneal macrophages after a 10-min period in 2-cm dishes. (n = 5 wild-type mice, n = 8 *ApoE*<sup>-/-</sup> mice, n = 8 *CGRP*<sup>-/-</sup> mice, and n = 4 *ApoE*<sup>-/-</sup>:*CGRP*<sup>-/-</sup> mice). (i) Representative photomicrographs showing migration of peritoneal macrophages into a scratch wound in a monolayer. Cells were observed immediately or 24 h after the scratch. Scale bar indicates 250 μm. (j) Migration of peritoneal macrophages in 96-well plate. (n = 6 wild-type mice, n = 5 *ApoE*<sup>-/-</sup> mice, n = 6 *CGRP*<sup>-/-</sup> mice, and n = 4 *ApoE*<sup>-/-</sup>:*CGRP*<sup>-/-</sup> mice). (k) Quantitative real-time RT-PCR analysis showing levels of *Tnfa* (n = 10 *ApoE*<sup>-/-</sup> mice, n = 9 *ApoE*<sup>-/-</sup>:*CGRP*<sup>-/-</sup> mice, *p* = 0.0271) and *Il6* (n = 10 *ApoE*<sup>-/-</sup> mice, n = 9 *ApoE*<sup>-/-</sup>:*CGRP*<sup>-/-</sup> mice, *p* = 0.1198) in mice peritoneal macrophages. Each bar indicates the mean ± SEM. \**p* < 0.05. Two-way ANOVA multiple comparisons with Tukey's post hoc test. If a statistical interaction was observed between factors, comparison of all four groups was performed by Tukey's post hoc test. Welch's t-test (k).

## Results

### CGRP deficiency exacerbates atherosclerosis in ApoE knockout mice

To evaluate the impact of CGRP on atherosclerosis, we compared lesion sizes in the aortas of wild-type, *CGRP*<sup>-/-</sup>, *ApoE*<sup>-/-</sup> and *ApoE*<sup>-/-</sup>:*CGRP*<sup>-/-</sup> mice following chronic HFD treatment. All groups were subjected to a HFD beginning at 5 weeks of age and continuing for 10 weeks (Fig. 1a). Using Oil Red O staining, we analyzed lesion development in the aortic arch of each mouse group. Our findings indicate that extensive atherosclerotic lesions occurred in both *ApoE*<sup>-/-</sup> and *ApoE*<sup>-/-</sup>:*CGRP*<sup>-/-</sup> mice after 10 weeks of HFD exposure (Fig. 1b). We divided the Oil Red O-staining aorta into three parts segment: the arch area, thoracic area, and abdominal area. Notably, the average size of plaques in the aortic arch areas of the *ApoE*<sup>-/-</sup>:*CGRP*<sup>-/-</sup> group was approximately 1.4 times larger than that in the *ApoE*<sup>-/-</sup> group (Fig. 1c). Furthermore, plaque development was observed in the arch area of *CGRP*<sup>-/-</sup> mice, which was greater than in the thoracic area and abdominal area (Fig. 1c–e). However, the lesion sizes in both the thoracic and abdominal areas are almost same when comparing *ApoE*<sup>-/-</sup> and *ApoE*<sup>-/-</sup>:*CGRP*<sup>-/-</sup> group (Fig. 1d,e). An increase in lipid deposition in the arch area was observed in *CGRP*<sup>-/-</sup> mice and *ApoE*<sup>-/-</sup>:*CGRP*<sup>-/-</sup> mice, suggesting that CGRP plays a role in the development of atherosclerosis. Analysis of hematoxylin and Oil Red O-staining sections showed an increase in atherosclerotic plaque size in both *ApoE*<sup>-/-</sup> and *ApoE*<sup>-/-</sup>:*CGRP*<sup>-/-</sup> group (Fig. 1f). Building on our findings that CGRP depletion induces atherosclerosis, we further explored the functional role of peritoneal macrophages in this process. Consequently, we switched to administering a high-fat diet for one week to assess macrophage function, as we determined that evaluating their function would be too late after 10 weeks of treatment, by which time atherosclerosis would have fully progressed. Given the pivotal role of macrophage foam cell formation in the early stages of atherosclerosis, as outlined by Glass et al.<sup>16</sup>, we hypothesized that macrophage functions might be altered in the context of early-stage atherosclerosis induced by HFD. To test this, we administered a 1-week HFD to wild-type, *CGRP*<sup>-/-</sup>, *ApoE*<sup>-/-</sup> and *ApoE*<sup>-/-</sup>:*CGRP*<sup>-/-</sup> mice, anticipating the onset of early pathological changes associated with atherosclerosis (Fig. 1g). Initial experiments focused on macrophage adherence, where we observed no significant difference between the groups (Fig. 1h). Subsequently, we employed a scratch wound assay to assess macrophage migration. Macrophages from both groups of mice fed a 1-week HFD demonstrated migration into the cell-free area (Fig. 1i), with the response in *CGRP*-deficient mice being approximately 1.7 times that of the control group (Fig. 1j). To further understand the impact of CGRP deficiency on inflammatory responses, we quantified mRNA expression levels of inflammatory markers *Tnfa* and *Il6* in the peritoneal macrophages of these mice. Our findings demonstrate a marked elevation in *Tnfa* expression levels but not *Il6* levels in *ApoE*<sup>-/-</sup>:*CGRP*<sup>-/-</sup> mice (Fig. 1k).

### Influence of CGRP on RAW 264.7 macrophage function and cytokine levels

Following our observation of increased migratory functions in *CGRP*-deficient peritoneal macrophages, we investigated the impact of exogenous CGRP on macrophage functionality using the mouse macrophage cell line RAW 264.7. Our study reveals that CGRP treatment did not significantly affect cell adherence (Fig. 2a). However, a dose-dependent decrease in macrophage migration was observed following treatment with CGRP at concentrations of 50 nM and 100 nM compared with the control group (0 nM) (Fig. 2b). Additionally, we observed a significant reduction in *Tnfa* mRNA expression levels in RAW 264.7 cells treated with 100 nM CGRP, whereas *Il6* levels remained unchanged (Fig. 2c).

### TNF-α inhibitor etanercept reduces the progression of atherosclerosis in *ApoE*<sup>-/-</sup>:*CGRP*<sup>-/-</sup> mice

Given the notably elevated *Tnfa* mRNA levels in peritoneal macrophages of *ApoE*<sup>-/-</sup>:*CGRP*<sup>-/-</sup> mice and observed reduction of *Tnfa* following CGRP administration, we next evaluated the therapeutic potential of the TNF-α inhibitor etanercept during early progression of atherosclerotic lesions. To evaluate the impact of etanercept on atherosclerosis, we needed to determine the duration of high-fat diet administration. Previous reports have indicated that chronic treatment with etanercept alone does not affect lipid deposition in LDL receptor-knockout mice<sup>17</sup>, leading us to explore earlier stages of the condition. The results in Fig. 1i showed a significant increase



in TNF $\alpha$  due to CGRP deficiency after one week of high-fat diet, so we initially administered the diet for one week. However, since no lipid deposition was observed in the aortic arch, we extended the administration to two weeks, at which point lipid deposition was observed (Fig. 3a). Therefore, we decided to conduct the evaluation of the early effects of the drug on atherosclerosis with two weeks of high-fat diet administration (Fig. 3b). After 2 weeks of etanercept administration, we observed no significant changes in serum lipid profiles [including total cholesterol and low-density lipoprotein (LDL) cholesterol] compared with the human IgG-administered control group (Fig. 3c). Analysis of Oil Red O-stained sections showed a decrease in atherosclerotic plaque size following etanercept treatment (Fig. 3d). To conduct a more detailed analysis, we divided the aorta into three segments. We observed no significant changes in the arch area (Fig. 3e). In the thoracic area, there was a tendency for a decrease following etanercept treatment (Fig. 3f). However, a substantial reduction in the size of atherosclerotic

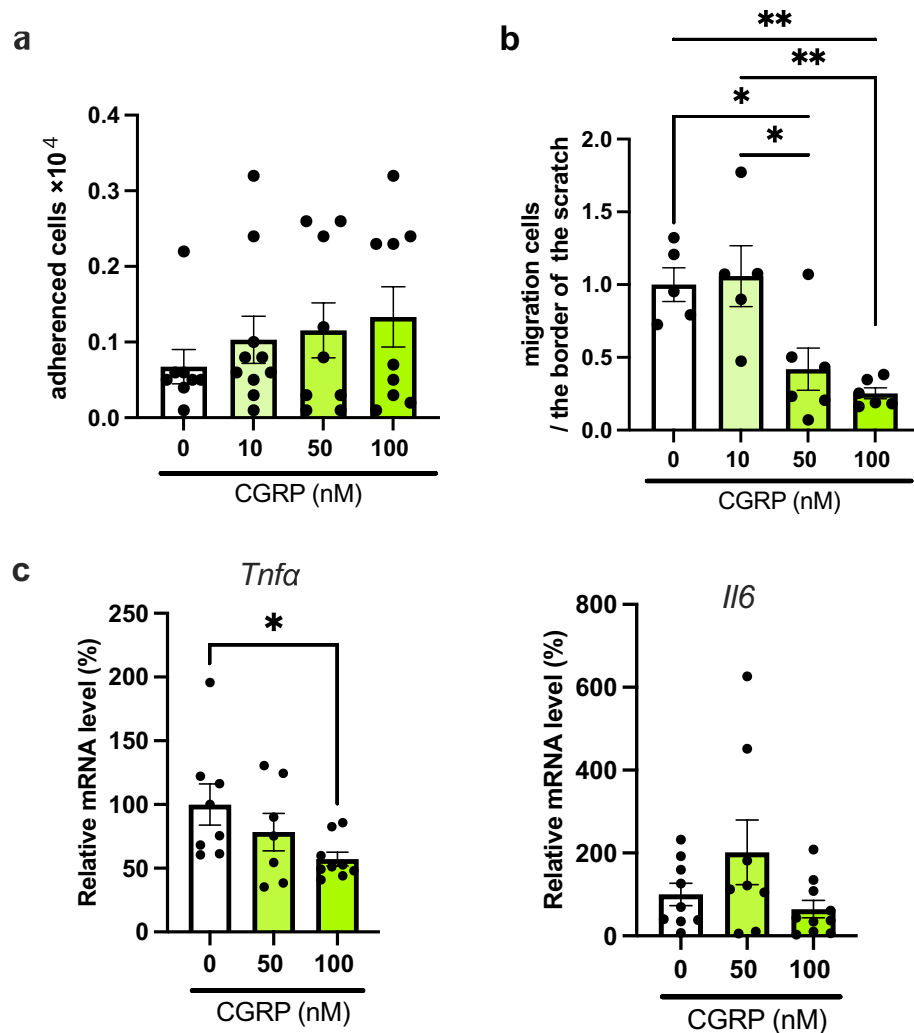


**Figure 2.** Effects of CGRP treatment on RAW 264.7 mouse macrophage cell line. (a) Number of adherent RAW 264.7 macrophages with CGRP administration (0, 10, 50, and 100 nM,  $n = 8, 10, 9$  and  $9$  respectively),  $F(3, 32) = 0.6382$ . (b) Migration of RAW 264.7 macrophage cell line in 96-well plate with CGRP administration (0, 10, 50, and 100 nM,  $n = 5, 5, 6$  and  $6$  respectively),  $F(3, 18) = 8.942$ . (c) Quantitative real-time RT-PCR analysis showing levels of *Tnfa* (0, 50, and 100 nM,  $n = 8, 7$  and  $9$  respectively,  $F(2, 21) = 3.187$ ) and *Il6* (0, 50, and 100 nM,  $n = 9, 8$  and  $10$  respectively,  $F(2, 24) = 2.426$ ). Each bar indicates the mean  $\pm$  SEM. \* $p < 0.05$ , \*\* $p < 0.01$ . One-way ANOVA with Tukey's test.

plaques was noted in the abdominal area (Fig. 3g). Additionally, *ApoE*<sup>-/-</sup>:*CGRP*<sup>-/-</sup> mice treated with etanercept displayed a marked reduction in the extent of plaques in the aortic root (Fig. 3h,i). To further understand the effect of TNF- $\alpha$  on macrophage migratory functions, a scratch wound assay was employed. The results indicate a significant reduction in macrophage migration in *ApoE*<sup>-/-</sup>:*CGRP*<sup>-/-</sup> mice treated with etanercept (Fig. 3j).

### Effects of CGRP inactivation using galcanezumab in *ApoE*<sup>-/-</sup> mice on atherosclerosis progression

Given the exacerbated atherosclerosis phenotype of *ApoE*<sup>-/-</sup>:*CGRP*<sup>-/-</sup> mice, we further investigated whether inactivation of CGRP via administration of the humanized monoclonal CGRP antibody galcanezumab to *ApoE*<sup>-/-</sup> mice would yield similar outcomes (Fig. 4a). Initially, to determine whether administration of the CGRP antibody affected systemic blood pressure in mice, we conducted weekly blood pressure measurements. No significant change in systolic blood pressure was observed compared with the IgG-treated control group (Fig. 4b). Following 2 weeks of galcanezumab treatment, we detected no notable changes in serum lipid profiles, including total cholesterol and LDL cholesterol, compared with the human IgG-administered group (Fig. 4c). Analysis of Oil Red O-stained sections showed a decrease in atherosclerotic plaque size following galcanezumab treatment (Fig. 4d). To conduct a more detailed analysis, we divided the aorta into three segments. We observed no significant changes in the arch area, thoracic area and abdominal area (Fig. 4e–g). However, in the thoracic area, there was a tendency for an increase following galcanezumab treatment (Fig. 4f). Additionally, both plaque areas and macrophage functions in the aortic root showed a slight increase following galcanezumab treatment (Fig. 4h–j).

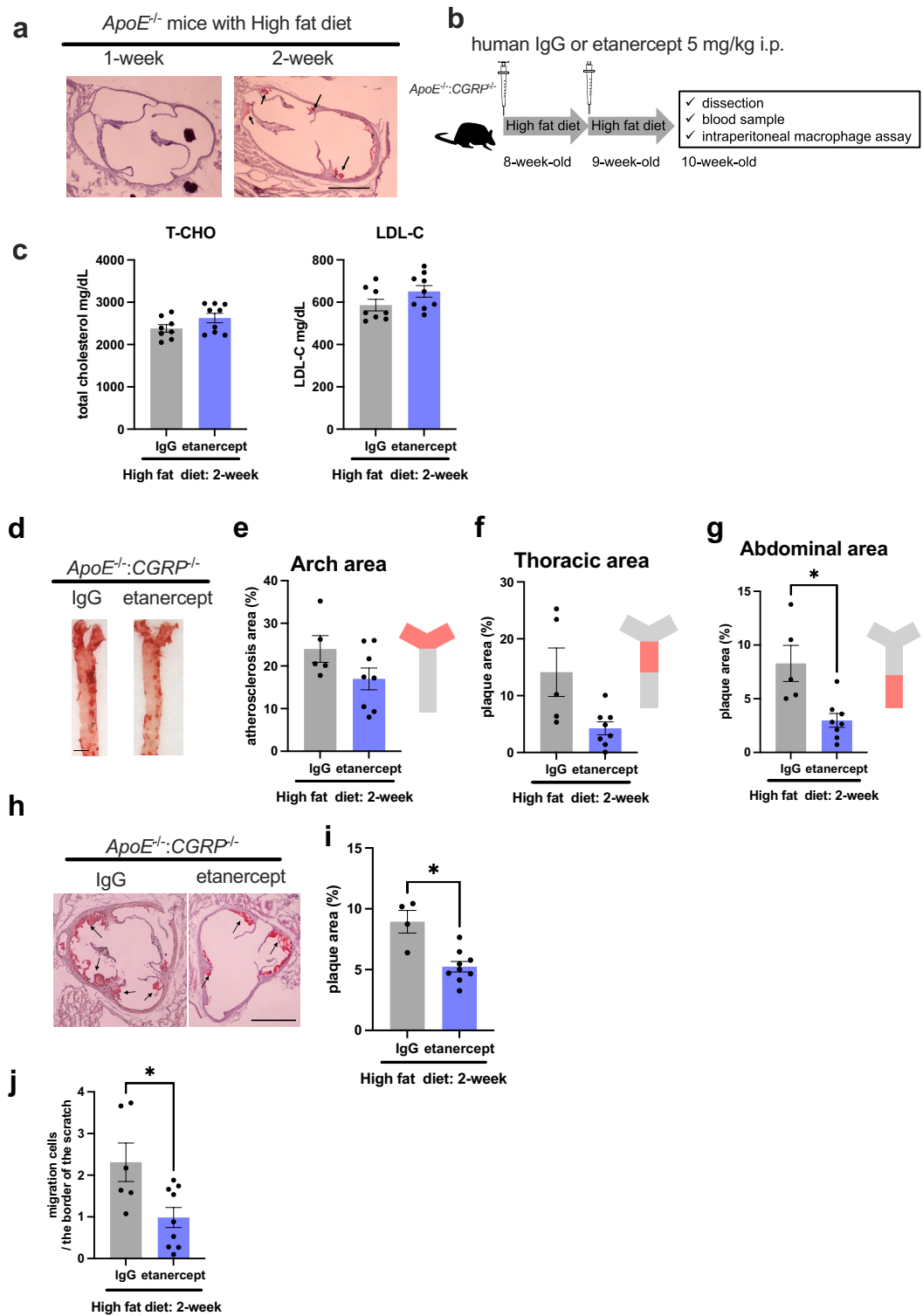


**Figure 3.** Etanercept treatment attenuates atherosclerotic lesions in *ApoE*<sup>-/-</sup>:*CGRP*<sup>-/-</sup> mice. (a) Administering a high-fat diet (HFD) to *ApoE*<sup>-/-</sup> mice and evaluating time-dependent lipid deposition at the aortic root with Oil Red O staining. (b) Eight-week-old *ApoE*<sup>-/-</sup>:*CGRP*<sup>-/-</sup> mice were fed a HFD for 2 weeks and human IgG or etanercept (5 mg/kg) was administered intraperitoneally once a week. (c) Serum levels of total ( $p=0.1081$ ) and LDL ( $p=0.116$ ) cholesterol after 2-week treatment ( $n=8$  IgG,  $n=9$  etanercept). (d) Representative photomicrographs of aortic lesions stained with Oil Red O from *ApoE*<sup>-/-</sup>:*CGRP*<sup>-/-</sup> mice. Scale bar indicates 2 mm. (e) Quantification of Oil Red O-stained plaque areas in the aortic arch ( $n=5$  IgG,  $n=8$  etanercept,  $p=0.118$ ). (f) Quantification of Oil Red O-stained plaques in the thoracic area ( $n=5$  IgG,  $n=8$  etanercept,  $p=0.0801$ ). (g) Quantification of Oil Red O-stained plaques in the abdominal area ( $n=5$  IgG,  $n=8$  etanercept,  $p=0.0306$ ). (h) Photomicrographs of aortic sinus lesions from *ApoE*<sup>-/-</sup>:*CGRP*<sup>-/-</sup> mice. Scale bar indicates 500  $\mu$ m. (i) Oil Red O-stained atherosclerotic plaques are quantified ( $n=4$  IgG,  $n=9$  etanercept,  $p=0.0192$ ) (j) Migration of mouse peritoneal macrophages ( $n=6$  IgG,  $n=9$  etanercept,  $p=0.0353$ ). Each bar indicates the mean  $\pm$  SEM. \* $p < 0.05$ , Welch's t-test.

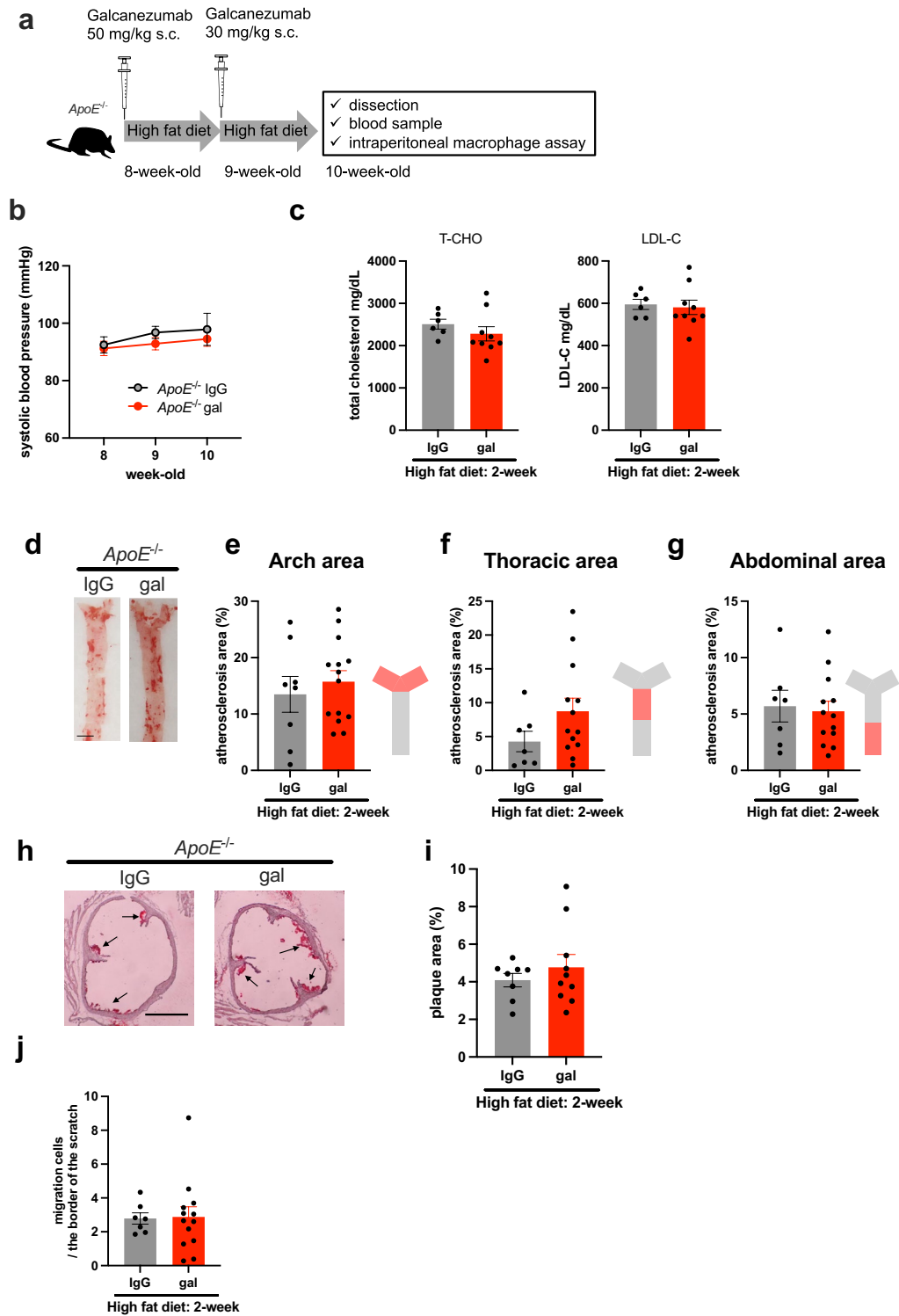


**Figure 4.** Effects of galcanezumab treatment on atherosclerotic lesions in *ApoE*<sup>-/-</sup> mice. (a) Eight-week-old mice were fed a high-fat diet (HFD) for 2 weeks and human IgG or galcanezumab were administered subcutaneously at an initial dose of 50 mg/kg, followed by a dose of 30 mg/kg in the second week. (b) Changes in systolic blood pressure and (c) serum levels of total (p=0.2882) and LDL cholesterol (p=0.7442) after 2-week treatment (n=6 IgG, n=9 galcanezumab). (d) Representative photomicrographs of aortic lesions stained with Oil Red O from *ApoE*<sup>-/-</sup> mice. Scale bar indicates 2 mm. (e) Quantification of Oil Red O-stained plaque areas in the aortic arch (n=7 IgG, n=13 galcanezumab, p=0.5577). (f) Quantification of Oil Red O-stained plaques in the thoracic area (n=7 IgG, n=13 galcanezumab, p=0.0849). (g) Quantification of Oil Red O-stained plaques in the abdominal area (n=7 IgG, n=13 galcanezumab, p=0.7882). (h) Photomicrographs of aortic sinus lesions from *ApoE*<sup>-/-</sup> mice. Scale bar indicates 500 μm. (i) Oil Red O-stained atherosclerotic plaques are quantified (n=8 IgG, n=10 galcanezumab, p=0.1952) (f) Migration of mouse peritoneal macrophages. (n=7 IgG, n=13 galcanezumab, p=0.451). Each bar indicates the mean ± SEM. \*p<0.05 Two-way analysis of variance followed by Sidak's post-test (b). Welch's t-test (c–j).

## Discussion

The primary goal of this study was to determine whether deletion of CGRP significantly alters atherosclerosis in ApoE-knockout mice. We observed that CGRP deficiency exacerbates atherosclerosis in *ApoE*<sup>-/-</sup> mice. Additionally, we found that CGRP suppressed *Tnfa* expression in RAW 264.7 macrophages. The TNF- $\alpha$  inhibitor etanercept reduced the progress of atherosclerosis. Recent studies similarly demonstrated that LPS-induced release of TNF- $\alpha$  was inhibited by CGRP treatment in RAW 264.7 macrophages<sup>18</sup> and inhibits inflammation<sup>19</sup>. Thus, CGRP is considered an important neuropeptide that can reduce excessive inflammation.

A previous study reported that exogenous CGRP influences pro-inflammatory cytokines in the RAW 264.7 macrophage cell line, noting upregulation of IL-1 $\beta$ , TNF- $\alpha$ , and IL-6 but not IL-10 levels following exposure to LPS<sup>18</sup>. In our current study, we ascertained that neither CGRP deficiency nor its administration significantly alters the level of *Il6*, although substantial changes were observed in *Tnfa* levels. These findings indicate that the influence of CGRP on IL-6 expression is relatively minor. Predominantly produced by macrophages and certain lymphocytes, TNF- $\alpha$  plays a pivotal role in regulating inflammatory responses, infection defense, and cellular apoptosis. Moreover, its involvement in macrophage proliferation makes it a significant contributor to atherogenesis<sup>20</sup>. Elevated TNF- $\alpha$  levels in the blood of older adults have been correlated with increased atherosclerosis prevalence<sup>21</sup>. In addition, TNF- $\alpha$  has been identified as a regulator of premature atherosclerosis in children with thalassemia, highlighting its role in arteriosclerosis irrespective of age<sup>22</sup>. Previous studies present conflicting findings regarding the role of TNF- $\alpha$  in atherosclerosis. Administration of etanercept to 60-week-old LDL receptor-knockout mice for 12 weeks did not result in plaque reduction<sup>17</sup>. However, treatment of 6-week-old K/BxAg7 mice, a model for arthritis/atherosclerosis, with etanercept for 13 weeks showed improvement of atherosclerosis<sup>23</sup>. These discrepancies might be attributable to the age of mice used in the studies. In our research, we administered etanercept to 8-week-old mice for a period of 2 weeks. Our findings suggest that etanercept may be more effective in early-stage lesions rather than chronic inflammatory conditions, whereby atherosclerosis progresses rapidly. We also demonstrated that in vitro, CGRP suppresses *Tnfa* production by both peritoneal macrophages and RAW 264.7 cells. Ma et al. previously reported that 100 nM CGRP suppressed TNF- $\alpha$  in RAW 264.7 cells with or without LPS stimulation<sup>18</sup>, consistent with our results.

Macrophages are well recognized as key regulators in the formation of atherosclerotic plaques<sup>24</sup>. The present study provides direct evidence that CGRP deficiency enhances macrophage migration and exacerbates atherosclerotic lesions in *ApoE*<sup>-/-</sup> mice. Previous research showed that attenuating macrophage migration can ameliorate atherosclerosis, particularly when targeting specific factors. For instance, neuropeptide Y deficiency reportedly increases macrophage migration via matrix metalloproteinase 8 (*MMP8*), contributing to plaque formation<sup>25</sup>. Additionally, Erk1/2 inhibitors<sup>25</sup> and the plant-based flavonoid alpinetin have been observed to inhibit macrophage migration, with the latter slowing atherosclerosis progression in *ApoE*<sup>-/-</sup> mice<sup>26</sup>. CGRP reportedly inhibits the Erk1/2 signaling pathway, thereby reducing vascular smooth muscle cell proliferation and migration<sup>27</sup>. Additionally, TNF- $\alpha$  increases Erk1/2 levels in endothelial cells<sup>28</sup> and induces Erk1/2 regulation in neonatal necrotizing enterocolitis model cells<sup>29</sup>. Therefore, we propose that CGRP could suppress macrophage migration by inhibiting the Erk1/2 pathway, thereby reducing TNF- $\alpha$  activity. However, further studies are necessary to confirm this hypothesis and fully understand the underlying molecular interactions.

Galcanezumab, a humanized IgG4 monoclonal antibody targeting CGRP, received United States Food and Drug Administration approval for migraine treatment in 2018. Our study found that galcanezumab seems to exacerbate early atherosclerotic lesions in *ApoE*<sup>-/-</sup> mice, marking this as the first study to explore its impact on atherosclerosis development. Similarly, a recent study identified increased risk for myocardial infarction in patients treated for 11 months with erenumab, another monoclonal antibody for CGRP<sup>30</sup>. However, in clinical trials, 6-month treatment with galcanezumab produced no significant changes in blood pressure, pulse, or electrocardiogram parameters<sup>31</sup>. Consistently, our findings indicate no significant change in systolic blood pressure with galcanezumab administration in *ApoE*<sup>-/-</sup> mice, aligning with previous clinical data. Studies of blood pressure in mouse models with permanent deletion of the CGRP gene are still debatable. Lu et al. reported that  $\alpha$ CGRP-lacking mice exhibit similar levels of cardiovascular function (including blood pressure) as control mice<sup>32</sup>. In contrast, Gangula et al. showed that  $\alpha$ CGRP-deletion mice had higher blood pressure than wild-type mice<sup>33</sup>. Notably, the method for blood pressure measurements was different in each study. Increased blood pressure in CGRP-deficient mice was measured by a catheter inserted into the carotid artery or a noninvasive tail cuff system<sup>33,34</sup>, while normotensive studies performed measurement by carotid or femoral artery catheterization and tail cuff<sup>32,35,36</sup>. Our study used tail cuff and obtained normal blood pressure measurements in *ApoE*<sup>-/-</sup> mice treated with galcanezumab. A previous study of blood pressure during temporary suppression of CGRP by administration of the CGRP receptor antagonist CGRP8-37 to normotensive rats did not change mean arterial pressure<sup>37</sup>. In contrast, CGRP8-37 administration to deoxycorticosterone-salt hypertensive or pregnant rats significantly increased blood pressure<sup>37,38</sup>. Although the function of CGRP on blood pressure regulation is still debatable, we speculate that CGRP depletion does not necessarily increase blood pressure, although CGRP might play a compensatory role to attenuate high blood pressure.

This study did have some limitations. The primary issue concerned the impact of CGRP deficiency on the quantity of macrophages within lesions. It is crucial to determine whether genetic deficiency of CGRP, produced by macrophages, influences macrophage levels. Additionally, the effects of CGRP deficiency on macrophages could be more precisely assessed by evaluating various parameters, such as chemotactic stimuli using a Boyden chamber and adhesion to endothelial cell monolayers.

The role of CGRP in atherosclerosis appears complex. Atherosclerosis progression involves inflammation and CGRP may have the potential to suppress this inflammatory process. In the present study, we demonstrated that the absence of CGRP could induce the progression of atherosclerosis. While there is still limited literature on the impact of galcanezumab administration on atherosclerosis, further investigation is warranted. At present, it can

be concluded that galcanezumab does not affect blood pressure, but caution is necessary regarding its potential effects on atherosclerosis.

## Methods

### Animals

All animal procedures were carried out in accordance with the Guide for the Care and Use of Laboratory Animals as published by the Japanese Association for Laboratory Animal Science, which complies with the ARRIVE guidelines and U.S. National Institutes of Health (NIH) Guide for the Care and Use of Laboratory Animals. All experiments were approved by the Animal Care and Use Committee of the Okayama University of Science (Authorization No. 2021-003). According to these guidelines, efforts were made to minimize the number of animals used and their suffering. A total of 141 male mice were used in this experiment. Mice were housed in groups of four or five per cage (23.5 × 35.3 × 16.0 cm, width × length × height) with a paper roll for environmental enrichment. Food [high-fat diet (HFD; F2HFD1, Oriental Yeast Co., Ltd, Tokyo Japan) 7.5% cocoa butter, 0.5% cholic acid, 1.25% cellulose, 1.0% mineral mix, 1.625% cellulose, 0.125% choline chloride, 1.25% cholesterol, 7.5% milk casein, 1.0% vitamin mix, 1.625% sucrose, 1.625% dextrin, 3.0% lard and 72% CRF-1 (standard mouse diet)] and water were available ad libitum. All animals were housed in the Animal Research Center of Okayama University of Science at a controlled ambient temperature of 22 °C with 50% ± 10% relative humidity and a 12-h light/dark cycle (lights on at 7:00 AM).

### Generation of *ApoE*<sup>-/-</sup>:*CGRP*<sup>-/-</sup> double-knockout mice

*CGRP*<sup>-/-</sup> mice on a C57BL/6 background were crossed with *ApoE*<sup>-/-</sup> mice on a C57BL/6 background, and F2 mice were genotyped to obtain *ApoE*<sup>-/-</sup>:*CGRP*<sup>-/-</sup> double-knockout mice homozygous for both the *CGRP* mutant allele and the *ApoE* mutant allele. *CGRP*<sup>-/-</sup> mice, which were knockout for the alpha isoform of CGRP were obtained from RIKEN Bioresource Research Center (#RBRC04109). To confirm *CGRP* knockout, tail-tip DNA was isolated and subjected to PCR as previously published<sup>39</sup>. For *ApoE* genotyping, primers used were those specified by Jackson Laboratories (ME, USA).

### Analysis of atherosclerosis

Mice were deeply anesthetized with sodium pentobarbital (100 mg/kg i.p.). After the aorta had been perfused with 10 mM phosphate-buffered saline (PBS; pH 7.4) via the left ventricle, it was removed by cutting off the minor branching arteries. After the adventitial and adipose tissue were removed, the aorta was fixed in 10% formalin for 20 min. After washing with PBS, aortas were cut open longitudinally and stained with Oil Red O. The extent of atherosclerosis in the aorta was quantified by using ImageJ software (National Institutes of Health). Both the acquisition of aortic images and analysis of lesion areas were performed in a blinded manner.

### Histological analysis

The heart was explanted and fixed in 10% formalin. After PBS wash, the heart was embedded in O.C.T. compound (Sakura Finetek, Tokyo, Japan). Serial sections of the aortic root were mounted on slides. Sections (10 μm) were air-dried and Hematoxylin and Oil Red O-stained for analysis to observe the lipid accumulation changes. Following stained, sections were cover-slipped and observed under an optical microscope (Olympus IX50, Olympus, Tokyo, Japan).

### Biochemistry

Blood samples were collected from the cardiac puncture under light anesthesia (isoflurane). Samples were centrifuged at 4 °C and the resulting serum was stored at -65 °C until assayed for cholesterol levels. Levels of total (TC) and LDL (LDL-C) cholesterol in serum were measured by outsourcing the analysis to Fujifilm WAKO Chemicals.

### RNA extraction

Total RNA was extracted from macrophages, placed in RNeasy lysis buffer (Qiagen, Tokyo, Japan), and stored at -30 °C, in accordance with a previous report<sup>40</sup>. Primer sequences (Table 1) were designed by the authors. The threshold cycle values for target genes tumor necrosis factor α (*Tnfa*) and interleukin 6 (*Il6*), as well as the internal control gene (actin, *Actb*) were determined.

### Cell culture

Peritoneal macrophages of mice were collected by peritoneal lavage. Mice were euthanized with pentobarbital-Na (50 mg/kg) before the collection of macrophages. About 30 mice were used to isolate macrophages, with 1 × 10<sup>7</sup> cells collected from each mouse. RAW 264.7 macrophages (American Type Culture Collection, Summit

	Forward	Reverse
<i>Tnfa</i>	AGTTCATATGGCCAGACCCT	CACTGGTGGTTTGCTACGA
<i>Il6</i>	CTGGAGTACCATAGCTACCTGGA	GTATCTCTCTGAAGGACTCTGGC
<i>Act</i>	GGTCAGAAGGACTCCTATGTG	GGTGTGGTCCAGATCTTCTCC

**Table 1.** Oligonucleotide sequences for real-time PCR amplification.



Pharmaceuticals International Corporation, Japan) and primary macrophages were cultured in Dulbecco's Modified Eagle Medium (DMEM; Gibco Invitrogen, Tokyo, Japan) containing 10% fetal bovine serum (FBS, Gibco Invitrogen), 100 U/mL penicillin, and 100 µg/mL streptomycin (Gibco Invitrogen). Cells were maintained at 60%–70% confluency at 37 °C in a humidified incubator with 5% CO<sub>2</sub> and air. Throughout the experiments, all efforts were made to minimize suffering.

### Macrophage migration assay

A macrophage migration assay was performed according to previous reports<sup>41</sup>. One day after plating peritoneal macrophages in a 96-well culture plate ( $1 \times 10^6$  cells), the monolayer was scratched with a sterile 200-µL pipette tip and cells were incubated for a further 24 h to allow for migration into the cell-free area. We counted all cells in the scratch region at 0 (just after scratch) and 24 h. Obtained data were calculated as number of migrated cells = (number of cells at 24 h—number of cells at 0 h)/ border of the scratch (cm). RAW 264.7 macrophages were seeded at a density of  $1 \times 10^5$  cells in 24-well culture plates. After 24 h, the media was changed to DMEM containing 1% FBS and 10 µg/mL mitomycin C. Subsequently, the monolayer was scratched and cells were treated CGRP (0, 10, 50 and 100 nM) for 24 h. The medium was replaced every day with CGRP.

### Adhesion assay

The adhesion assay used a protocol modified from a previously reported method<sup>42</sup>. Peritoneal macrophages or RAW 264.7 macrophages were placed at a density of  $1 \times 10^6$  cells in 40-mm culture dishes and allowed to attach for 10 min. Thereafter, the wells were washed with PBS and cells that attached were detached by 0.05% trypsin and counted.

### Drug treatments

To investigate the effects of TNF-α, we administered etanercept (Pfizer Japan Inc.) or normal human IgG (Fuji Film WAKO Japan) at a dose of 5 mg/kg intraperitoneally once a week for 2 weeks to *ApoE*<sup>-/-</sup>:*CGRP*<sup>-/-</sup> mice. To evaluate the efficacy of a CGRP antibody, we used galcanezumab. During the first week of drug administration, 50 mg/kg of galcanezumab (Eli Lilly Japan K.K.) or human IgG was subcutaneously administered to *ApoE*<sup>-/-</sup> mice; the following week, 30 mg/kg was administered subcutaneously<sup>43</sup>.

### Statistical analysis

All data are expressed as the mean ± standard error of the mean (SEM). GraphPad Prism 10 software (GraphPad Software Inc., San Diego, CA, USA) was used for all statistical analyses. Comparisons between two values were analyzed using Welch's t-test. Analysis of variance (ANOVA) followed by Tukey's multiple comparison test was used to determine statistical significance where appropriate. Two-way ANOVA was also performed when comparing four values. If there was a significant difference in the interaction between groups, Tukey's post hoc test was used to compare all groups. When performing a comparison of time series, we used Sidak's post-test. A p value < 0.05 was considered statistically significant.

### Data availability

Numerical source data for figures can be found in Supplementary Data 1.

Received: 13 February 2024; Accepted: 2 August 2024

Published online: 08 August 2024

### References

- Brain, S. D., Williams, T. J., Tippins, J. R., Morris, H. R. & MacIntyre, I. Calcitonin gene-related peptide is a potent vasodilator. *Nature* **313**, 54–56 (1985).
- Amara, S. G., Jonas, V., Rosenfeld, M. G., Ong, E. S. & Evans, R. M. Alternative RNA processing in calcitonin gene expression generates mRNAs encoding different polypeptide products. *Nature* **298**, 240–244 (1982).
- Jacobs, J. W. *et al.* Calcitonin messenger RNA encodes multiple polypeptides in a single precursor. *Science* **213**, 457–459 (1981).
- Hoovers, J. M. *et al.* High-resolution chromosomal localization of the human calcitonin/CGRP/IAPP gene family members. *Genomics* **15**, 525–529 (1993).
- O'Connor, T. P. & van der Kooy, D. Enrichment of a vasoactive neuropeptide (calcitonin gene related peptide) in the trigeminal sensory projection to the intracranial arteries. *J. Neurosci.* **8**, 2468–2476 (1988).
- Tsai, S. H., Tew, J. M., McLean, J. H. & Shipley, M. T. Cerebral arterial innervation by nerve fibers containing calcitonin gene-related peptide (CGRP): I. Distribution and origin of CGRP perivascular innervation in the rat. *J. Comp. Neurol.* **271**, 435–444 (1988).
- Zhou, Y. *et al.* Calcitonin gene-related peptide reduces Porphyromonas gingivalis LPS-induced TNF-α release and apoptosis in osteoblasts. *Mol. Med. Rep.* **17**, 3246–3254 (2018).
- Tsujikawa, K. *et al.* Hypertension and dysregulated proinflammatory cytokine production in receptor activity-modifying protein 1-deficient mice. *Proc. Natl. Acad. Sci. U. S. A.* **104**, 16702–16707 (2007).
- Schneider, L. *et al.* Protective effects and anti-inflammatory pathways of exogenous calcitonin gene-related peptide in severe necrotizing pancreatitis. *Pancreatology* **9**, 662–669 (2009).
- Zhang, X. *et al.* Inhibitory effects of calcitonin gene-related peptides on experimental vein graft disease. *Ann. Thorac. Surg.* **90**, 117–123 (2010).
- Singh, Y. *et al.* Calcitonin gene-related peptide (CGRP): A novel target for Alzheimer's disease. *CNS Neurosci. Ther.* **23**, 457–461 (2017).
- Libby, P., Lichtman, A. H. & Hansson, G. K. Immune effector mechanisms implicated in atherosclerosis: From mice to humans. *Immunity* **38**, 1092–1104 (2013).
- Wang, Y. *et al.* TRPV1 agonism inhibits endothelial cell inflammation via activation of eNOS/NO pathway. *Atherosclerosis* **260**, 13–19 (2017).

14. Zhang, C., Ye, L., Zhang, Q., Wu, F. & Wang, L. The role of TRPV1 channels in atherosclerosis. *Channels (Austin)* **14**, 141–150 (2020).
15. Tam, L.-S., Kitas, G. D. & González-Gay, M. A. Can suppression of inflammation by anti-TNF prevent progression of subclinical atherosclerosis in inflammatory arthritis?. *Rheumatology* **53**, 1108–1119 (2014).
16. Glass, C. K. & Witztum, J. L. Atherosclerosis. The road ahead. *Cell* **104**, 503–516 (2001).
17. Park, K.-Y. & Heo, T.-H. Critical role of TNF inhibition in combination therapy for elderly mice with atherosclerosis. *Cardiovasc. Ther.* <https://doi.org/10.1111/1755-5922.12280> (2017).
18. Ma, W., Dumont, Y., Vercauteren, F. & Quirion, R. Lipopolysaccharide induces calcitonin gene-related peptide in the RAW264.7 macrophage cell line. *Immunology* **130**, 399–409 (2010).
19. Duan, J.-X. *et al.* Calcitonin gene-related peptide exerts anti-inflammatory property through regulating murine macrophages polarization in vitro. *Mol. Immunol.* **91**, 105–113 (2017).
20. Branch, D. R., Turner, A. R. & Guilbert, L. J. Synergistic stimulation of macrophage proliferation by the monokines tumor necrosis factor-alpha and colony-stimulating factor 1. *Blood* **73**, 307–311 (1989).
21. Bruunsgaard, H., Skinhøj, P., Pedersen, A. N., Schroll, M. & Pedersen, B. K. Ageing, tumour necrosis factor-alpha (TNF-alpha) and atherosclerosis. *Clin. Exp. Immunol.* **121**, 255–260 (2000).
22. Ragab, S. M., Safan, M. A., Obeid, O. M. & Sherief, A. S. Lipoprotein-associated phospholipase A2 (Lp-PLA2) and tumor necrosis factor-alpha (TNF- $\alpha$ ) and their relation to premature atherosclerosis in  $\beta$ -thalassemia children. *Hematology* **20**, 228–238 (2015).
23. Rose, S. *et al.* A novel mouse model that develops spontaneous arthritis and is predisposed towards atherosclerosis. *Ann. Rheum. Dis.* **72**, 89–95 (2013).
24. van Gils, J. M. *et al.* The neuroimmune guidance cue netrin-1 promotes atherosclerosis by inhibiting the emigration of macrophages from plaques. *Nat. Immunol.* **13**, 136–143 (2012).
25. Wu, W. *et al.* NPY promotes macrophage migration by upregulating matrix metalloproteinase-8 expression. *J. Cell. Physiol.* **236**, 1903–1912 (2021).
26. Dong, D., Zhang, Y., He, H., Zhu, Y. & Ou, H. Alpinetin inhibits macrophage infiltration and atherosclerosis by improving the thiol redox state: Requirement of GSK3 $\beta$ /Fyn-dependent Nrf2 activation. *FASEB J.* **36**, e22261 (2022).
27. Qin, X.-P. *et al.* Effect of calcitonin gene-related peptide on angiotensin II-induced proliferation of rat vascular smooth muscle cells. *Eur. J. Pharmacol.* **488**, 45–49 (2004).
28. Cao, Y., Zhang, J., Meng, X. & Wang, D. TNF- $\alpha$  induces early growth response gene-1 expression via ERK1/2 activation in endothelial cells. *Acta Diabetol.* **50**, 27–31 (2013).
29. Yuan, Y. *et al.* TNF- $\alpha$  induces autophagy through ERK1/2 pathway to regulate apoptosis in neonatal necrotizing enterocolitis model cells IEC-6. *Cell Cycle* **17**, 1390–1402 (2018).
30. Perino, J. *et al.* Myocardial infarction associated with erenumab: A case report. *Pharmacotherapy* **42**, 585–589 (2022).
31. Oakes, T. M. *et al.* Evaluation of cardiovascular outcomes in adult patients with episodic or chronic migraine treated with galcanezumab: Data from three phase 3, randomized, double-blind, placebo-controlled EVOLVE-1, EVOLVE-2, and REGAIN studies. *Headache* **60**, 110–123 (2020).
32. Lu, J. T. *et al.* Mice lacking alpha-calcitonin gene-related peptide exhibit normal cardiovascular regulation and neuromuscular development. *Mol. Cell. Neurosci.* **14**, 99–120 (1999).
33. Gangula, P. R. R. *et al.* Increased blood pressure in  $\alpha$ -calcitonin gene-related peptide/calcitonin gene knockout mice. *Hypertension* **35**, 470–475 (2000).
34. Mai, T., Wu, J., Diedrich, A., Garland, E. M. & Robertson, D. Calcitonin gene related peptide (CGRP) in autonomic cardiovascular regulation and vascular structure. *J. Am. Soc. Hypertens.* **8**, 286–296 (2014).
35. Skaria, T. *et al.* Blood pressure normalization-independent cardioprotective effects of endogenous, physical activity-induced  $\alpha$ CGRP ( $\alpha$  calcitonin gene-related peptide) in chronically hypertensive mice. *Circ. Res.* **125**, 1124–1140 (2019).
36. Argunhan, F. *et al.* Calcitonin gene-related peptide protects against cardiovascular dysfunction independently of nitric oxide in vivo. *Hypertension* **77**, 1178–1190 (2021).
37. Supowit, S. C., Zhao, H., Hallman, D. M. & DiPette, D. J. Calcitonin gene-related peptide is a depressor of deoxycorticosterone-salt hypertension in the rat. *Hypertension* **29**, 945–950 (1997).
38. Gangula, P. R. R., Dong, Y. L., Wimalawansa, S. J. & Yallampalli, C. Infusion of pregnant rats with calcitonin gene-related peptide (CGRP)(8–37), a CGRP receptor antagonist, increases blood pressure and fetal mortality and decreases fetal growth. *Biol. Reprod.* **67**, 624–629 (2002).
39. Oh-hashii, Y. *et al.* Elevated sympathetic nervous activity in mice deficient in  $\alpha$ CGRP. *Circ. Res.* **89**, 983–990 (2001).
40. Hashikawa, N., Ido, M., Morita, Y. & Hashikawa-Hobara, N. Effects from the induction of heat shock proteins in a murine model due to progression of aortic atherosclerosis. *Sci. Rep.* **11**, 7025 (2021).
41. Yang, J.-X. *et al.* Synergistic effect of phosphodiesterase 4 inhibitor and serum on migration of endotoxin-stimulated macrophages. *Innate Immun.* **24**, 501–512 (2018).
42. Wang, Z. *et al.* Silence of TRIB3 suppresses atherosclerosis and stabilizes plaques in diabetic ApoE $^{-/-}$ /LDL receptor $^{-/-}$  mice. *Diabetes* **61**, 463–473 (2012).
43. Johnson, K. W. *et al.* Characterization of transit rates in the large intestine of mice following treatment with a CGRP antibody, CGRP receptor antibody, and small molecule CGRP receptor antagonists. *Headache* **62**, 848–857 (2022).

## Acknowledgements

We thank Edanz (<https://jp.edanz.com/ac>) for editing a draft of this manuscript.

## Author contributions

N.H.-H. designed the experiments; N.H., S.I., and N.H.-H. conducted the experiments; N.H.-H. wrote the main manuscript text; N.H., and N.H.-H. conducted the statistical analyses and prepared the figures. All authors reviewed and approved the manuscript.

## Funding

Wesco Science Foundation 2024 supported this work.

## Competing interests

The authors declare no competing interests.

## Additional information

**Supplementary Information** The online version contains supplementary material available at <https://doi.org/10.1038/s41598-024-69331-5>.

**Correspondence** and requests for materials should be addressed to N.H.-H.

**Reprints and permissions information** is available at [www.nature.com/reprints](http://www.nature.com/reprints).

**Publisher's note** Springer Nature remains neutral with regard to jurisdictional claims in published maps and institutional affiliations.

**Open Access** This article is licensed under a Creative Commons Attribution-NonCommercial-NoDerivatives 4.0 International License, which permits any non-commercial use, sharing, distribution and reproduction in any medium or format, as long as you give appropriate credit to the original author(s) and the source, provide a link to the Creative Commons licence, and indicate if you modified the licensed material. You do not have permission under this licence to share adapted material derived from this article or parts of it. The images or other third party material in this article are included in the article's Creative Commons licence, unless indicated otherwise in a credit line to the material. If material is not included in the article's Creative Commons licence and your intended use is not permitted by statutory regulation or exceeds the permitted use, you will need to obtain permission directly from the copyright holder. To view a copy of this licence, visit <http://creativecommons.org/licenses/by-nc-nd/4.0/>.

© The Author(s) 2024